Spatial and Temporal Analysis of a Tidal Floodplain Landscape—Amapá, Brazil—Using Geographic Information Systems and Remote Sensing

Valeria F.G. Pereira, Russell G. Congalton, and Daniel J. Zarin

Abstract

*For at least 12,000 years, Amazonian floodplains (*várzea*) have been exploited by human populations. Although they represent a small fraction of the Amazon basin, floodplains contain the most productive ecosystems of the region. Easy access and the abundance of valuable forest products have historically led to higher human population densities and higher resource use than in many interfluvial areas. Recent research has brought attention to land-use and land-cover change in upland Amazonian forests, but relatively little research has been conducted on similar dynamics in the floodplains.*

In this project, we used photointerpretation of 1970s aerial photographs and digital image classification of Landsat Thematic Mapper (TM) 5 imagery from the 1990s to produce land-cover maps used for change detection analysis. A study area in the tidal floodplains of the State of Amapá, in the northern Brazilian Amazon, was evaluated. The accuracy of the Landsat TM classification and errors inherent to the techniques used were assessed. Several changes in the study site were observed, including increases in the areal extent of secondary growth and palm forests and corresponding decreases in intact várzea *forest area.*

Introduction

In recent decades, large-scale forest clearing and burning to establish agricultural fields and cattle ranching have brought international attention to the Brazilian Amazon. The extensive destruction of tropical forests impacts carbon cycling on a global scale (Onis, 1992; Skole and Tucker, 1993) and reduces biodiversity (Nepstad *et al.*, 1992; Gallopin and Winograd, 1995). These are only the most recent and most obvious effects of human manipulation in this region.

Covering about 2 percent of the Brazilian Amazon, floodplain environments (*várzea*) have been the most intensively used ecological zone in the Amazon basin (Pires, 1974; Anderson, 1991). First occupied by Indians (Roosevelt, 1991; Roosevelt, 1995), resource use in this landscape was originally limited to fishing, hunting, and fruit extraction. Between 2000 and 4000 years ago, slash and burn cultivation was established. The arrival of Europeans in the sixteenth century brought commercial logging (Anderson *et al.*, 1992). At present, logging, agriculture, cattle ranching, mining, hunting, fishing, and extraction of non-timber products are the dominant resource uses in this region. These activities produce changes in vegetation patterns across the landscape. Although logging and extraction of non-timber products affect forest composition, the activities that produce the most obvious changes in the environment are mechanized agriculture, mining and cattle ranching.

Natural and human-induced disturbances in the Amazon have been detected using Landsat Thematic Mapper (TM) imagery (Skole and Tucker, 1993; Brondizio *et al.*, 1994; Nelson, 1994). However, the use of Landsat imagery for Amazonian floodplains has been limited due to the almost continuous cloud cover in much of this environment (Sippel *et al.*, 1994). Catalogs of Landsat MSS and TM imagery distributed by the Brazilian Institute of Space Research (INPE) reported that only a few usable Landsat images exist for the floodplains of the State of Amapá. This lack of imagery has limited the investigation of these environments. The use of aerial photographs for mapping and change detection studies of the tropical environment is not as common. This is partly because of the difficulty and/or high cost of obtaining and processing such photography. Aerial photography provides higher spatial resolution, and often more cloud-free data, than does satellite imagery. Existing aerial photography allows investigation of changes for periods in which there is no satellite imagery.

The purpose of this research was to identify and quantify natural and human-induced changes in a tidal floodplain in the state of Amapá from 1976 to 1995. The state of Amapá is in the northern Brazilian Amazon, and about 10 percent of its land area consists of floodplains (IBGE, 1994). The floodplains (*várzea*) of Amapá consist of various vegetation cover classes and include flooded forests, grasslands, palm forests, and secondary growth. Floodplains on the Atlantic coast also include mangrove ecosystems.

The specific objectives of this research were (1) to produce land-cover maps based on the interpretation and classification of aerial photos from the 1970s and Landsat imagery from the 1990s, (2) to quantify historical changes in vegetation cover based on these maps, and (3) assess the accuracy of digital classification for vegetation mapping in the Amazonian flood-

V.F.G. Pereira and R.G. Congalton are with the Department of Natural Resources, University of New Hampshire, Durham, NH 03824 (russ.congalton@unh.edu).

D.J. Zarin is with the School of Forest Resources and Conservation, University of Florida, Gainesville, FL 32611

Photogrammetric Engineering & Remote Sensing
Vol. 68, No. 5, May 2002, pp. 463–472.

0099-1112/02/6805–463$3.00/0

plains. This project involved a combination of digital processing of Landsat Thematic Mapper images, visual classification (interpretation) of aerial photography, and the use of GIS analysis techniques.

Literature Review

This literature review is divided into two parts. The first section presents background material about the Amazon floodplain. The second section deals with the spatial analyses used in this project including aerial photointerpretation/photogrammetry, remote sensing, geographic information systems (GIS), and change detection.

Human Impacts on the Amazon Floodplain

The economic extraction of natural resources in this region is seasonal, and depends upon the flooding regime, which affects the reproductive cycle of species (e.g., exploitation of *açaí* fruits during the dry season), and access for harvesting (e.g., extracting wood during the wet season). The first saw and veneer mills were established in the Amazon estuary in the 1950s (Barros and Uhl, 1995). Since then, due to the increased demand for softwood in the national and international market, selective logging of *Virola surinamensis* (*virola*) has been one of the most important activities in this area.

Virola is a fast growing, shade-intolerant species that flourishes on disturbed sites (Macedo and Anderson, 1993). Consequently, the high density of these trees in some sites has been associated with past disturbances. Current logging practices result in significant ecological changes including decreased number of saplings, decreased basal area, loss of germplasm, and changes in the understory. Extensive extraction of *virola*, once a dominant species in this region, has led to significant declines in the population and, potentially, its long-term viability. Harvesting of several of the *várzea* timber species is increasing (Barros and Uhl, 1995). In the study area, the most important of these at present is Calycophyllum spruceanum (Benth), locally known as *pau mulato* (Applegate *et al.*, 2000; Pinedo-Vasquez *et al.*, 2001).

The agricultural potential of Amazonian floodplains has been increasingly stressed because of the region's fertile soils and the need to decrease the conversion of upland forests to agriculture use (Prance, 1979). However, the physical characteristics of floodplain soils coupled with the severe flooding regime and oxygen constraints may limit this potential. Tidal floodplain agriculture in the region focuses on maize and rice but also includes beans and other annuals and semi-perennials. Agricultural plots are often concurrently managed for future timber and/or palm production and are only rarely completely abandoned following the decline of maize and/or rice production (Pinedo-Vasquez *et al.*, 2001). Zarin *et al.* (1998) suggest that soil nutrient status is little affected by traditional shifting cultivation in the tidal floodplains.

Palm heart extraction began in the estuary in the 1970s. Many of the processed palm hearts consumed throughout the world are derived from the *açaí* palm (*Euterpe oleracea* Mart.), which grows abundantly in floodplain forests of the Amazon estuary. The exploitation of palm heart in certain places has been intensive and as a result the average palm heart today is smaller than it was 20 years ago, meaning that smaller, younger stems are being cut today. However, the *açaí* palm is well suited for management because of its abundance, rapid growth, and multi-stemmed life form. Under proper management, palm hearts can be harvested from the same clump over many years through controlled thinning (Pollak *et al.*, 1995).

Several edible fruits are collected in this region, both for local consumption and for the external market (Peters, 1992). *Açaí* (*Euterpe oleracea* Mart) is the most consumed. Locals also consume the fruits of other palms. *Buriti* (*Mauritia Flexuosa*), *patauá* (*Jessenia bataua*), and *bacaba* (*Oenocarpus* sp.) are the most common. The fruits of *buriti*, which are commonly consumed by humans elsewhere in Amazonia, are used primarily as food for pigs in the study area. Over-exploitation of *açaí* may decrease the productivity of the species, as well as reduce its regeneration.

Natural grasslands, which serve as breeding grounds for many species, are increasingly converted to pasture (Goulding *et al.*, 1996). Grazing affects the structure of the soils by causing soil compaction, and increasing erosion (Junk, 1989).

Spatial Analyses

Aerial photography has long been established as a tool for land-cover and land-use mapping, for forest classification, and for monitoring spatial-temporal changes (Paine, 1981; Campbell, 1987). High resolution and low cloud cover are some of its advantages over other sources of remotely sensed data. However, the high cost of the aerial photographic missions coupled with the smaller area covered by them has limited its use when planning environmental research for large areas such as the Amazon Basin.

The importance of digital remotely sensed imagery such as Landsat Multispectral Scanner (MSS) and Thematic Mapper (TM) for environmental analysis has been well described in the literature, and widely used to document deforestation, and land-cover and land-use change, in the Amazon. High cloud cover in the Basin has been a critical obstacle for high frequency and large-scale coverage. This problem is especially significant in the region of the State of Amapá, where the breeze from the ocean creates an almost continuous cloud cover. One solution to this problem is to use active remote sensing devices such as RADAR. Numerous studies have been conducted in the Amazon flooplain using active sensors (e.g., Hess *et al.* (1995) and Sippel *et al.* (1998)). However, our study only used conventional aerial photographs and Landsat TM satellite imagery.

Despite its myriad of uses, remote sensing has limitations and inherent errors that may be introduced during pre-processing, digital and visual classification, rectification to real world coordinates, post-processing and registration to other images (Lillesand and Kiefer, 1994). Still, it is the best source of information available today and can be used to develop detailed maps of the rate and geographical extent of deforestation in tropical forests, and thus document their location and expansion over time (Skole *et al.*, 1994).

Change detection analysis is a technique which performs a comparison between land-cover classifications from different dates (e.g., post-classification technique) or by simultaneous analysis of multi-temporal data (Jensen, 1995). In the post-classification approach, images and/or aerial photographs of different dates are classified independently and then the classifications are compared. In the simultaneous analysis of multi-temporal data, the comparison may be of individual pixel values from different dates or it may be performed by simultaneously classifying images from different dates.

Post-classification techniques may be used to compare the classification of aerial photographs from one date to a classification of digital remotely sensed data from another date. These classifications can be compared either visually or digitally. Several studies have been developed using GIS and remote sensing techniques to compare different classifications (e.g., the NASA Pathfinder project).

Change detection analysis has been performed for large areas of the Amazon region (e.g., INPE, 1990; Skole and Tucker, 1993), as well as for several smaller study sites (e.g., Brondizio *et al.*, 1994; Nelson, 1994). There has been little change detection analysis conducted in the State of Amapá, mainly due to the almost continuous cloud cover, which makes it difficult to monitor changes using any type of satellite imagery.

Methods

Study Area

The study area for this project is located in southeastern Amapá, in the Brazilian Amazon Basin, approximately between the latitudes 00° 03′ N and 00° 30′ S and longitudes 51° 13′ W and 51° 42′ W (Figure 1). A related analysis was also carried out at another site nearby and has been reported by Zarin *et al.* (2002). The area is characterized by a mean annual temperature of 28° Celsius and two seasons: rainy season (January–June) and dry season (July–December). This area is relatively close to the mouth of the Amazon River. Although there is no influence of the salt water from the ocean, it is affected by the 2- to 3-meter tides characteristic of the Amazon estuary. Tidal floods occur diurnally and attain maximum amplitudes during the equinoxes. At the full and new moons, the most intensive floods occur during the March–April equinox, which coincides with the high levels of the rainy season.

The flooding regime affects the composition of the soils, which are primarily composed of dystrophic-to-eutrophic hydromorphic gley soils and eutrophic-dystrophic alluvial soils, depending upon soil texture and nutrient status (Projeto RADAM, 1974). These soils are characterized by a high clay content (Anderson and Ioris, 1992). The low porosity of the soils and the general lack of relief result in poor drainage and consequently low oxygen availability. These soil characteristics are reflected in the composition and structure of the native vegetation (Anderson, 1991).

Amazonian floodplain vegetation includes two major components: flooded forests (*mata de várzea*) and grasslands (*campos de várzea*) (Pires, 1974). A more detailed classification of flooded forest is given by Prance (1979). He proposed a key describing seven forest categories subjected to inundation based on vegetation cover, type of water, and the duration of flooding.

Field Data Collection

Two field trips were made to collect ground data in order to (1) obtain data for training in the classification process, (2) collect data for the accuracy assessment of the digital classification of Landsat TM data, and (3) georeference Landsat TM images and land-cover vector layers. An August 1996 trip was for field reconnaissance and acquisition of the data sets: maps, Landsat TM images, and aerial photos. The area was visited, ground control points (GCPs, using the Global Positioning System (GPS)) were obtained, training samples for the classifications and samples for the accuracy assessment were collected, pictures of the different environments were taken, and field maps were drawn. Also, general observations and notes were taken, including descriptions of the area and land uses employed by local inhabitants. The purpose of a second trip in March 1997 was to collect more GCPs and more training samples, to collect data for accuracy assessment, and to check the results obtained in the initial digital classification.

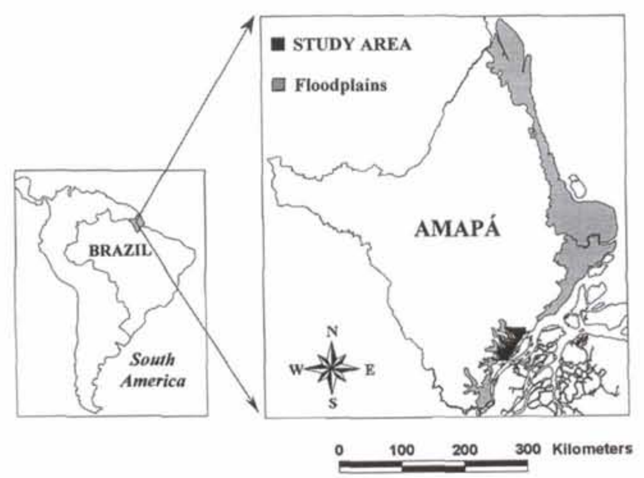

Figure 1. Map showing the State of Amapá, Brazil and the exact location of the study area.

Classification Scheme

A classification scheme was developed, and a classification key was produced in which five classes were identified (Table 1). A classification scheme consists of not only the names of the classes, but also the definitions of each class. The number of classes and the level of detail within each class depends upon the nature of the project. In order to be valid, there are two critical criteria that a classification scheme must meet: (1) classes must be mutually exclusive and (2) the classification system must be totally exhaustive (Congalton, 1991). In this project, classes were chosen that could be reliably identified on both aerial photography and Landsat satellite imagery.

Land-Cover Map from Photointerpretation

To map the study area, 35 black-and-white infrared aerial photos at a scale of 1:70,000 were used, and a land-cover map was produced by interpreting the effective area (i.e., center) of each photo. An analysis of the frequency of areas by class versus size of the areas mapped was performed to determine the appropriate minimum mapping unit (MMU). An MMU of 8100 m^2 (or approximately 3 by 3 TM pixels) was selected because of the scale of the aerial photographs (1:70,000). This was the minimum area in which all classes could be identified and distinguished on the photos. Due to the size of the study area to be mapped and the scale of the aerial photographs, the area was divided into sub-sections (i.e., each section covering two flight lines). A total of six sub-sections were mapped.

Land-Cover Map from Landsat TM Imagery

A subset of the Landsat Thematic Mapper 5 (TM5)-path 225, row 60, for 26 September 1995-covering the study area was used to perform supervised and unsupervised classification. The same classification scheme was used as with the photointerpretation. ERDAS IMAGINE Version 8.2 for Microsoft Windows NT and

Table 1. The Land-Cover Classification Scheme Used for Mapping both the Aerial Photography and the Landsat Thematic Mapper Satellite Imagery

Class	Description
Water + Unvegetated Banks	This class includes water bodies in general (rivers, streams, and lakes) and unvegetated banks which are affected by tidal flooding.
Herbaceous Cover	This class includes grasslands in general, herbaceous vegetation along rivers and streams, small agricultural fields, and pastures.
Secondary Growth	This class includes areas which have undergone exploitation of wood and palm hearts, abandoned agricultural fields and pastures, and areas in the contact between different ecosystems (e.g., transitional forests or ecotones).
Palms	This class includes stands of palm trees mainly represented by stands of *Mauritia Flexuosa*, commonly known as *buriti* or *miriti*, and by stands of *Euterpe Oleracea*, commonly known as *açaí*.
Várzea Forest	This class includes forests subjected to inundation, both tidal and seasonal *várzea*, which are composed of large trees and are rich in palms.

also the Version 8.2 for UNIX were used to process this imagery. The digital image processing was carried out in five steps: rectification, data exploration, classification, post-processing, and accuracy assessment.

The first step of this project was to geometrically correct the image to UTM coordinates using GPS points acquired during the field data collection. The nearest-neighbor resampling algorithm was used because it does not alter the pixel values (Lillesand and Kiefer, 1994). A total of 12 GPS points were used for the geometric rectification.

Before any data exploration procedures were performed, the image was masked using the outside boundary of the photointerpreted land-cover map to reduce computer storage, increase system performance, and decrease spectral variation throughout the scene. Clouds and shadows present on the 1995 Landsat imagery were also eliminated from the data set by masking. Data exploration techniques such as principal component analysis, divergence analysis, ratios, and histogram equalization were utilized. After producing new derivative bands (i.e., ratios and principal components), spectral pattern analysis and divergence techniques were used to choose the best bands to be used in the classification process. Two approaches for classifying the images were tested: unsupervised classification and supervised classification.

A sub-sample of the ground data collected during the field data collection was used for training areas in the supervised classification. Ten signatures were generated for each class. Divergence and spectral pattern analyses were applied to choose the bands that best discriminated between classes. After the bands were chosen, supervised classification using the maximum-likelihood algorithm was performed.

Several attempts to classify the Landsat TM images were made using unsupervised classification. These attempts included variations in number of clusters and spectral bands. The clusters identified in the images were labeled based on information from the field data collection.

Filters are commonly used as a post-processing technique to reduce speckle and to smooth classified images. In this project, the MMU defined for the photointerpretation was 8100 m^2, which corresponds to nine 30- by 30-meter pixels (3 by 3). It is critical for the change detection analysis to be able to directly compare the land-cover map generated from the 1970s aerial photos with the map derived from the 1990s Landsat TM imagery. Therefore, filters were applied to the digital classifications as a way to normalize the spatial resolution and make them comparable to the land-cover map derived from the photointerpretation. Different kernel sizes were tested (3 by 3, 5 by 5, and 7 by 7), and a comparison of the size of the areas before and after the application of these filters was performed to define which filter should be used.

The last step in the process was to assess the accuracy of the land-cover map derived from the Landsat imagery. In order to perform this assessment, a total of 262 sampling areas were acquired. Established accuracy assessment procedures were performed to validate and to choose the best classification. Error matrices were generated to calculate the overall, user's, and producer's accuracies (Story and Congalton, 1986). Kappa analysis was also performed to test and compare different errors matrices and determine which was best (Congalton, 1991; Congalton and Green, 1999).

Geographic Information System Analysis

In this project, the GIS analysis was divided into three major steps: (1) digitizing of the land-cover map produced using photointerpretation of the aerial photos, (2) georeferencing the photo interpreted land-cover map, and (3) conversion of the digitized vector map to raster format. In the first step, the set of six polygons overlays (i.e., the six subsections previously mentioned) created by photointerpretation were digitized into a GIS, i.e., PC ARC/INFO Version 3.4.2b (ESRI, 1994). The second step was to georeference these data to the Universal Transverse Mercator (UTM) geographic reference system. GPS points collected during the field data collection and ground control points calculated from a topographic map were used to georeference the data set. Next, the subsections were edge-matched to produce one single map of the study area. The last step was to convert the vector layers from vector format to a raster format. This process was performed using Arc Info GRID Version 7.0.3 for UNIX. The grid cells were defined as 30 by 30 meters to match the Landsat TM resolution. After the grid layers were created, they were imported into IMAGINE (ERDAS, 1995) Version 8.2 to produce the raster map of the study area and to perform the change detection.

Change Detection

The post-processing change detection technique was used to perform the temporal analysis in this study. First, the land-cover map generated from photointerpretation was rasterized using GRID (ESRI, 1994), imported into IMAGINE (ERDAS, 1995) as an image file, and then registered to the corresponding filtered land-cover map generated from the digital image classification. The registration was performed using the nearest-neighbor resampling algorithm. After registration, the two land-cover maps were overlayed and the change detection was performed (Brondizio *et al.*, 1994).

Results

Land-Cover Map from Photointerpretation

Table 2 presents the photointerpretation key developed for use with the aerial photographs. Plate 1a shows the land-cover map produced using this key by photointerpretation of the 1970's aerial photography.

Land-Cover Map from Landsat TM Imagery

The digital image processing used to create a land-cover map from the Landsat TM imagery was carried out in five steps: rectification, data exploration, classification, post-processing, and accuracy assessment.

Twelve GPS points were used to geometrically rectify the land-cover map to Universal Transverse Mercator (UTM) coordinates. These points were mostly concentrated in a small portion of the study area. To guarantee that the GCPs were spread evenly throughout the image, four additional points located in each corner of the image were obtained from a topographic map. A total RMS error of 0.30 pixels (approximately 9 meters) was achieved.

Attempts were made to visually distinguish between palms and intact forest before the digital classifications were performed. Several derivative bands were generated, analyzed, and compared using spectral pattern and divergence analysis. The bands that produced the best separation for intact forest and palms were bands 3 (red), 5 (middle infrared), and 7 (middle infrared) with the application of contrast stretching techniques.

Supervised classification was performed using ten training areas for each land-cover class. The maximum-likelihood algorithm was used to label all the pixels. Unsupervised classification was performed with a varying number of clusters. The results of both classification approaches were evaluated by generating error matrices and running a Kappa analysis to statistically determine which land-cover map was best. The land-cover map generated using the unsupervised classification approach is presented in Plate 1b.

The resulting classified image contained areas less than the MMU (3 by 3 pixels) defined for creating the land-cover map from the photointerpretation. Small groupings of pixels and single pixels (speckling) are an artifact of the spatial resolution

TABLE 2. KEY FOR THE VISUAL INTERPRETATION OF AERIAL PHOTOS

Class #	Class	Tone	Texture	Shape
10	Várzea Forest	From light to medium gray	Rough. The canopy seems to have several layers with dominant trees.	Irregular
30	Herbaceous Cover	From medium to dark gray	Smooth. Appears to be flat.	Irregular. However it sometimes may have straight edges.
50	Palms	Light to medium gray	Rough. It may have different canopy heights. It looks like small rough balls close together.	Irregular
70	Secondary Growth	Medium gray	Rough. Vegetation appears sparce. The height of trees appears to be lower than in flooded forest.	Irregular, mostly forming stripes along forest or grassland.
90	Water + Unvegetated Banks*	Dark gray to black *Light gray	Smooth	Rivers, streems, or lakes. *Irregular mainly along river shores.

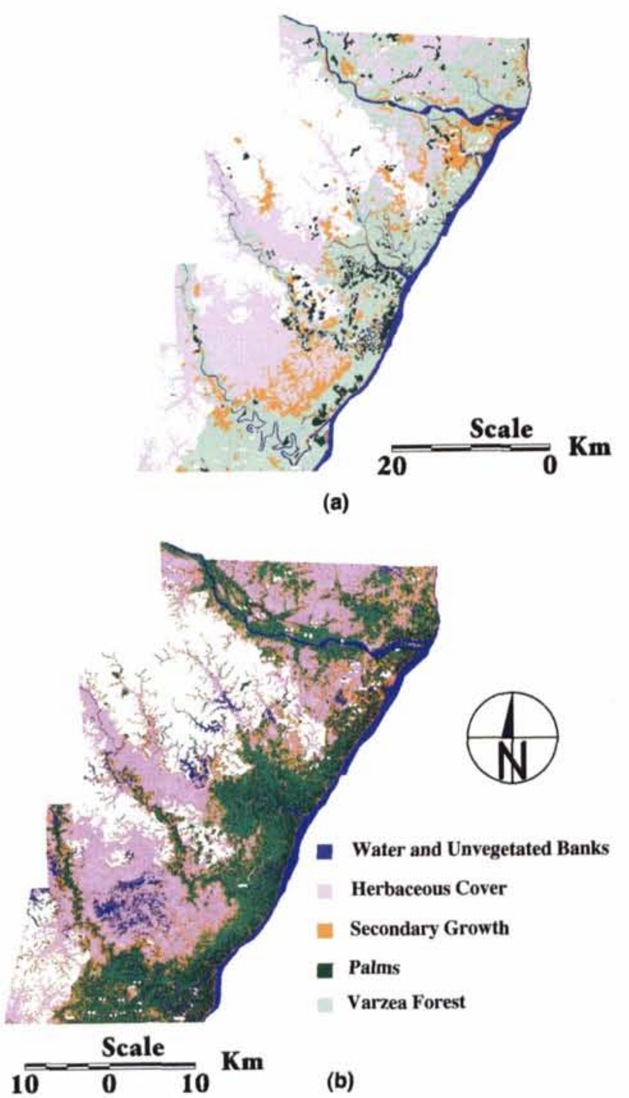

Plate 1. (a) Land-cover map produced using photointerpretation of aerial photos taken in the 1970s. (b) Land-cover map of unsupervised classification of Landsat TM5 imagery of 1995.

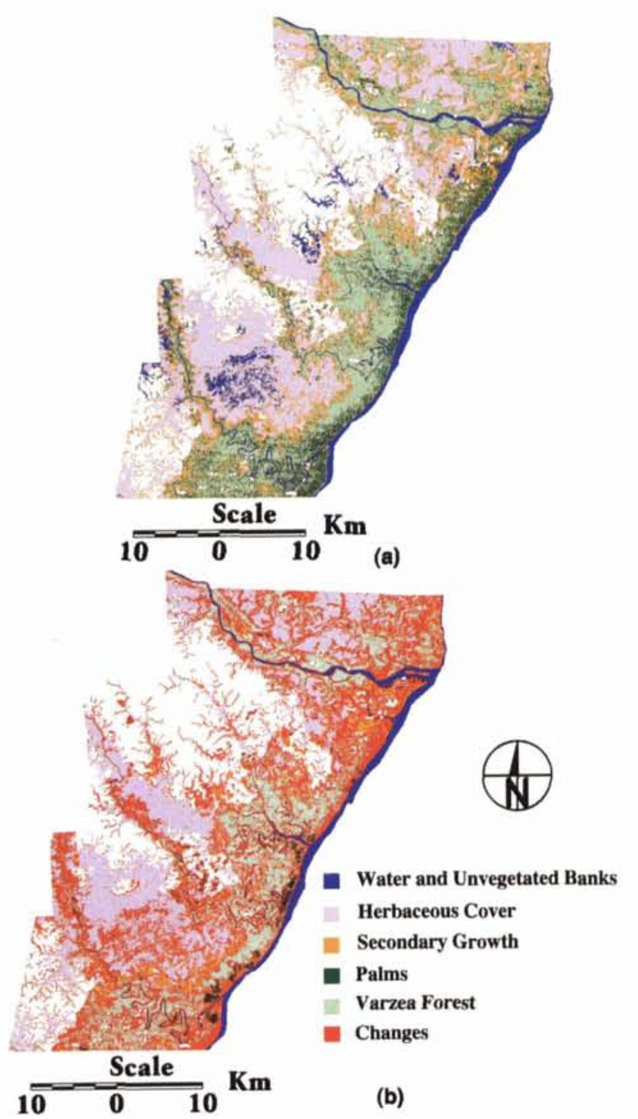

Plate 2. (a) Land-cover map of unsupervised classification using a 3 by 3 majority filter applied only to the class palms. (b) Land-cover change map with the unchanged areas mapped as the land-cover class and the changed areas mapped in red.

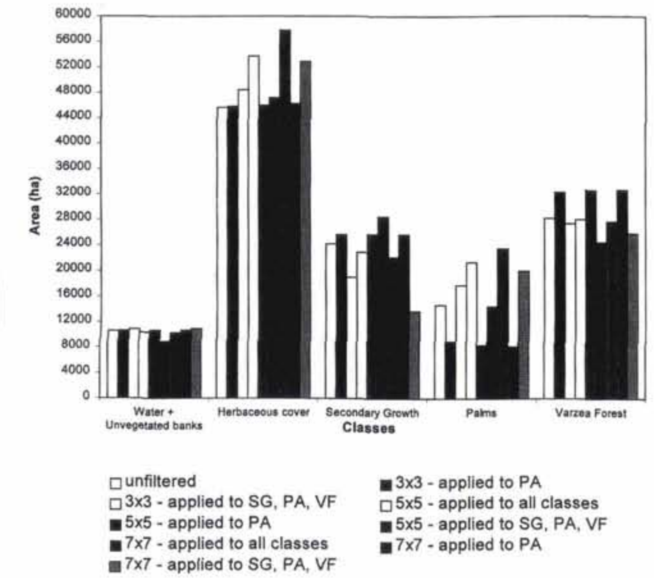

Figure 2. Comparison of areas by class before and after the application of various majority filters (SG = Seconday Growth, PA = Palms, and VF = Várzea Forest).

and spectral characteristics of digital data. On the aerial photos, especially the small scale (1:70,000) photos, areas less than the MMU were not identified. On the imagery, speckling was observed mainly in areas of palms, which was the hardest class to identify. In other words, the photointerpretation tends to lump areas together as polygons, while the image processing tends to split the area apart into pixels. This problem could compromise the validity of the change detection analysis. Land covers that could have existed in the 1970s, but that were not identified from the photointerpretation because of photo scale and MMU issues, may be compared with areas clearly identified on the pixel-based Landsat TM imagery of the 1990s. Therefore, it would be very easy to overestimate the changes. The solution to this problem was the application of filters to eliminate the areas less than the MMU. Several filters of different kernel sizes and applied to different classes were compared and analyzed. The 3 by 3 majority filter applied only to palms was chosen for the final product because it mostly affected palms and intact forest and had little effect over the remaining classes (Figure 2). Plate 2a shows the map of the unsupervised classification with a majority filter applied only to the palms.

Table 3 presents the comparison of the distribution in hectares of land-cover classes for the photointerpreted land-cover map versus the unsupervised classification of Landsat TM scene before and after filtering. Intact forest decreased significantly in areal extent in the study area. The herbaceous cover also decreased its areal extent. Palms increased significantly even after the application of the majority filter.

Table 4. Error Matrix Showing Land-Cover Types for the Unsupervised Classification

		Reference					
	Class	WU	HC	SG	PA	VF	Total
Classified	WU	**50**					50
	HC		**44**	1			45
	SG		8	**48**	1	5	62
	PA			1	**46**	5	52
	VF			1	5	**47**	53
	Total	50	52	51	52	57	262

Classes:
WU—Water + Unvegetated Banks
HC—Herbaceous Cover
SG—Secondary Growth
PA—Palms
VF—Várzea Forest

Producer's Accuracy	**User's Accuracy**
WU = 50/50 = 100%	WU = 50/50 = 100%
HC = 44/52 = 85%	HC = 44/45 = 98%
SG = 48/51 = 94%	SG = 48/62 = 77%
PA = 46/52 = 88%	PA = 46/52 = 88%
VF = 47/57 = 82%	VF = 47/53 = 89%

Overall Accuracy = 235/262 = 90%
KHAT accuracy = 85.67%

The unsupervised classification using three bands (3, 5, 7) showed the highest overall accuracy—90 percent—and a KHAT accuracy of 85.67 percent (Table 4). The classification of the palms also had high producer's and user's accuracy. The results of the accuracy assessment of the filtered classified image were lower than those for the unfiltered classified image. The overall accuracy was 89 percent and the KHAT accuracy was 85.67 percent (Table 5). Supervised classification resulted in low overall accuracy. This may be due to spectral differences that could not be observed during the selection of training areas.

Change Detection

The land-cover map derived from interpretation of the 1970s aerial photos was overlayed with the filtered land-cover map generated from the Landsat TM imagery in order to perform the change detection. The RMS error obtained in this registration process was 16.9 meters. The change detection map is shown in Plate 2b. Herbaceous cover and intact forest decreased while the remaining classes increased in areal extent (Figure 3). The distributions (in hectares) of land-cover change are shown in Table 6. These results are presented in a contingency table in which the columns represent the 1995 satellite classification and the rows represent 1976 photointerpretation. Bold values along the major diagonal represent the areas unchanged from 1976 to 1995.

Approximately 55 percent of the area classified as water + unvegetated banks for the 1990s came from areas classified as water + unvegetated banks for the 1970s. The rest of this area for the 1990s is formed largely by areas classified on the aerial photos as herbaceous cover and intact forest. In other words,

Table 3. Distribution of the Land-Cover Classes from Visual Classification (VC) of the Aerial Photographs, and Unsupervised Classifications (UC) of the Landsat TM Scenes before and after a 3 by 3 Majority Filter Was Applied to the Areas Mapped as Palms

		Classes (Area in ha)					
		Water + Unvegetated Banks	Herbaceous Cover	Secondary Growth	Palms	Várzea Forest	Total
Classifications	VC-1976	7696	48800	12958	5399	48430	123283
	UC-1995 unfiltered	10578	45654	24159	14679	28213	123283
	UC-1995 filtered	10629	45776	25675	8881	32322	123283

TABLE 5. ERROR MATRIX SHOWING LAND-COVER TYPES FOR UNSUPERVISED CLASSIFICATION AFTER A 3 BY 3 MAJORITY FILTER WAS APPLIED TO THE AREAS MAPPED AS PALMS

	Reference						
	Class	WU	HC	SG	PA	VF	Total
Classified	WU	**50**					50
	HC		**46**	1			47
	SG		6	**47**	3	2	58
	PA				**40**	6	46
	VF			3	9	**49**	61
	Total	50	52	51	52	57	262

Classes:
WU—Water + Unvegetated Banks
HC—Herbaceous Cover
SG—Secondary Growth
PA—Palms
VF—Várzea Forest

Producer's Accuracy
WU = 50/50 = 100%
HC = 46/52 = 88%
SG = 47/51 = 92%
PA = 40/52 = 77%
VF = 49/57 = 86%

User's Accuracy
WU = 50/50 = 100%
HC = 46/45 = 98%
SG = 47/62 = 81%
PA = 40/52 = 87%
VF = 49/53 = 80%

Overall Accuracy = 232/262 = 89%
KHAT accuracy = 85.67%

about 55 percent of the existing area of water + unvegetated banks came from the same class and the remaining area came from all other classes, but the herbaceous cover and intact forest contributed much more than the secondary growth and palms.

Approximately 75 percent of the area classified as water + unvegetated banks in the aerial photos did not change. The remaining area has changed probably due to process of deposition along rivers and streams.

Approximately 80 percent of herbaceous cover did not change. Palms and water + unvegetated banks contributed a little to the area classified as herbaceous cover in the 1990s imagery. Secondary growth contributed almost 10 percent and the intact forest contributed about 10 percent.

The majority of the areas classified as herbaceous cover on the 1970s aerial photos remained unchanged (about 75 percent). The remaining area has become secondary growth (about 10 percent), intact forest (less than 10 percent), water + unvegetated banks (less than 10 percent), and palms (less than 5 percent).

Secondary growth is now composed of about 50 percent of areas that were classified as intact forest in the 1976s aerial photos. Less than 20 percent of the secondary growth came from the same category (unchanged) and approximately 30 percent came from the herbaceous cover. Together, the palms and water + unvegetated banks contributed less than 10 percent of the existing area of secondary growth. Most of the area

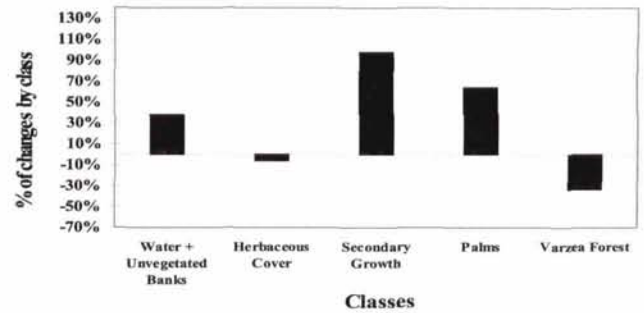

Figure 3. Percentage of land-cover changes by land-cover class.

classified as secondary growth in the 1970s photos became herbaceous cover and intact forest and a great amount remained unchanged (approximately 40 percent).

The majority of the area classified as palms in the 1990s imagery came from intact forest (approximately 70 percent). About 10 percent came from the palms (unchanged) and less than 10 percent of the palms in each sub-area came from other classes. About 20 percent of the areas classified as palms in the 1970s aerial photos did not change. It may be also observed that almost 50 percent of the area classified as palms in the 1970s has become intact forest. Less than 10 percent of the palms became water + unvegetated banks and between 10 percent and 20 percent has become herbaceous cover and secondary growth.

Almost 80 percent of the area classified as intact forest in 1990s imagery came from the same category in the 1970s photos. All other classes contributed with less than 10 percent. Approximately 60 percent of the areas classified as intact forest in the 1970s remained unchanged in the 1990s. About 30 percent of the 1970s intact forest classification has become secondary growth and the remaining 1970s intact forest area has become water + unvegetated banks, herbaceous cover, and palms.

Discussion

How dynamic and how stable are ecosystems belonging to environments subjected to inundation? How large are stands of palm trees? Are they expanding? How large are areas of natural grasslands? These are some of the questions addressed in this project. To answer these questions, the remotely sensed data must allow for the accurate characterization and delineation of the major existing ecosystems.

Land-Cover Map from Photointerpretation

Mapping from aerial photos presents several problems. The vertical aerial photos used were at a nominal scale of 1:70,000,

TABLE 6. DISTRIBUTION OF LAND-COVER CHANGES FOR THE STUDY AREA. THE ROWS REPRESENT THE 1976 LAND-COVER CLASS (DERIVED FROM PHOTOINTERPRETATION) AND THE COLUMNS REPRESENT THE 1991 COVER CLASS (DERIVED FROM THE LANDSAT TM IMAGERY). BOLD VALUES (I.E., THE DIAGONAL) REPRESENT THE AREAS UNCHANGED FROM 1976 TO 1995

		1995 Cover Classification (area in ha)					
	Class	Water + Unvegetated Banks	Herbaceous Cover	Secondary Growth	Palms	Várzea Forest	Total 1976
1976 Cover Classification (Area in ha)	Water + Unvegetated Banks	**5948**	194	581	367	607	7696
	Herbaceous Cover	3181	**37105**	6618	524	1373	48801
	Secondary Growth	347	4025	**5160**	870	2555	12957
	Palms	116	593	1160	**1076**	2453	5399
	Várzea Forest	1036	3860	12156	6043	**25333**	48429
	Total 1995	10629	45776	25674	8881	32322	123283

and were supposed to present minimum distortion, due to the flat topography of the region. The major problems observed during the interpretation and mapping using the aerial photos were:

- several flight lines had the percentage of side overlap less than 10 percent; therefore, some areas that needed to be mapped were outside of the effective area;
- some adjacent flight lines were taken at different dates and contained strong contrast variation; and
- the paper of the photos had a tendency to shrink, which increased the difficulty in matching the photos.

The first two problems are results of differences in flying height and atmospheric conditions and the third is a result of paper quality. As a solution for these problems, manual adjustments were used to produce the vector layers.

The aerial photos did not have a significant percentage of cloud cover; however, sun reflections in water bodies were observed in some photos. Blurred areas on some photos made it difficult to correctly identify and classify some areas. This error was evident, but could not be fixed or measured, because there was no accurate information available for the land cover for the 1970s. Therefore, it was impossible to evaluate how accurate the classifications in those areas were. However, through visual comparison of the maps, it was observed that the patterns of the land-cover classes were quite similar, both in spatial distribution and type of land cover.

Land-Cover Map from Landsat TM Imagery

Palm was the hardest class to identify; the spectral values were very close to the spectral values of the intact forest. In the unsupervised classification, areas of intact forest with palms, intact forest with high density of palms, and pure stands of palms were identified. These distinctions may be explained by differences in levels of biomass and water content that were identified using the near- and middle-infrared bands and were observed on the ground during the second field data collection, when the results of the initial classification were taken to the field. However, as the density of palms within flooded forest could not be observed on the photos, both types of forest were placed in a single class.

The use of a majority filter proved to be the best solution to solve the problem of overestimation of changes in palms. This filter was applied only to palms. When filters were applied to all classes, the areal extent of palms unexpectedly increased instead of decreasing. The area of herbaceous cover increased at the expense of secondary growth. The unfiltered classification can be used for identifying the actual land-cover distribution or the one closest to the actual distribution. However, it could not be used with the photointerpretation to measure spatial changes because of differences in spatial resolution and minimum mapping unit.

Filters with kernels of 3 by 3, 5 by 5, and 7 by 7 were tested. The 3 by 3 kernel was chosen based on the size of the MMU defined for photointerpretation. Even after the application of these majority filters, several speckles could still be observed in palms. An analysis of how these filters worked was performed, identifying areas of high frequency of pixels classified as palms before and after the filters were applied.

The field data acquired during the ground trip were carefully described in every detail. The photos and notes taken proved to be extremely useful for accuracy assessment, as well as in the definition of the classes and in the process of labeling clusters and defining training areas.

Several attempts were made to increase the accuracy of the mapping. Perhaps, utilization of more detailed ground information could increase the accuracy of these classifications. More extensive ground surveys, bigger samples, and more specific details (e.g., forest inventory of the samples, measurements of water content and canopy closure, amount of illumination in the understory and local reflectance, and leaf water content) could further refine the classification (Brondizio *et al.*, 1996).

Change Detection Analyses

Increases in the areal extent of secondary growth and palm forests and corresponding decreases in intact *várzea* forest area were the most salient features of the analysis. These changes are consistent with results we have previously reported for a nearby site (Zarin *et al.*, 2002) and are indicative of land-use patterns present in this region. The results permitted a more detailed analysis of the data in which every class was analyzed separately. Table 7 presents a summary of natural processes and human induced disturbances that may explain individual characteristics of changes detected.

Water + unvegetated banks increased 38 percent in the study area. Erosion processes may explain part of the area increased. It was observed that the majority of these changes were found along rivers and streams, where the flooding pattern results in high rates of erosion and deposition.

Most of the changes from herbaceous cover to water + unvegetated banks may be due to a higher flood level in the imagery versus the photos. This was the case for areas classified as herbaceous cover in the 1970s that were not found along major rivers. These were probably areas of natural grassland that are seasonally flooded. Herbaceous cover decreased 6 percent. The tendency of natural grasslands is to stay stable or to be replaced by the surrounding vegetation. Secondary growth increased 98 percent in the study area. The majority of the area gained by this class was intact forest, which may suggest intense exploitation of wood, as well as clearing and abandonment.

Palms increased 64 percent. This pattern may be explained by the characteristics of the palms as an indicator of human activities and as an early successional species. However, it may not mean that these areas are now covered by pure stands of *Mauritia flexuosa* or *Euterpe oleracea*. It may imply that the areal extent of palms in general has increased. Errors associated with palms may have originated with digital classification. The distance between the mean spectral value of palms and the mean spectral value of intact forest was small, which generated some confusion that can be observed in the error matrices. The use of contrast stretching techniques may have helped in separating large homogeneous stands of palms, in which there was little spectral influence of other factors (e.g., differences in age of the trees, spatial distribution, water content in soil, shades, etc.). However, the influence of mixed pixels and the diversity in species composition may have compromised the spectral separation of this class in smaller stands, as well as in stands with diverse species composition (mixed stands).

Intact forest decreased 33 percent. This class contributed the most to the increase in the remaining classes. This observation does not mean that the remaining areas classified as intact forest in the 1990s were all forest in the 1970s. In fact, 21.6 percent of the areas classified as intact forest in the 1990s came from other classes. Nonetheless, loss of intact forest greatly exceeds the rate of successional development for other classes. Overexploitation of forest products coupled with grazing are likely to be responsible for much of the loss of flooded *várzea* forest.

Conclusion

In this study, the major cover-class transitions observed were the loss of intact *várzea* forest and corresponding gains in the area of palm-dominated stands and secondary growth. These transitions correspond to prevalent patterns of resource extraction from the *várzea* (Zarin *et al.*, 2002). Removal of merchantable timber species from the *várzea* forest results in extensive damage to the forest canopy and the creation of a heterogeneous

TABLE 7. SUMMARY OF PROCESSES THAT COULD POTENTIALLY INFLUENCE THE CHANGES DETECTED

		1990s Cover Class				
	Class	Water + Unvegetated Banks	Herbaceous Cover	Secondary Growth	Palms	Várzea Forest
1970s Cover Class	Water + Unvegetated Banks	**Unchanged**	Deposition. Succession.	Deposition. Succession.	Deposition. Succession.	Deposition. Succession.
	Herbaceous Cover	Erosion	**Unchanged**	Succession.	Process of succession. Palms functioning as pioneer species.	Succession.
	Secondary Growth	Erosion	Human induced disturbances. Areas deforested for pasture, and agriculture.	**Unchanged**	Process of succession. Palms functioning as pioneer species.	Succession.
	Palms	Erosion	Human induced disturbances. Areas deforested for pasture, and agriculture. Exploitation of palm hearts.	Human induced disturbances. Exploitation of palm hearts.	**Unchanged**	Succession.
	Várzea Forest	Erosion	Human induced disturbances. Areas deforested for pasture, and agriculture.	Human induced disturbances. Selective logging.	Human induced disturbances. Selective logging, creating favorable environment for palms.	**Unchanged**

matrix of gaps which may be exploited by palms and other pioneer species. Harvesting of one of the palm species, *Euterpe oleraceae*, which is used in the palm-heart industry, can lead to further degradation of forest structure. The transition from *várzea* forest to either palms or secondary growth may occur as a result of a single event or season of forest exploitation, or the process may occur over a longer period of sustained resource extraction. As the results indicate, successional development of the palm and secondary growth cover classes to the intact forest class also occurs. During the interval measured in this study, however, the rate of intact forest loss clearly exceeded that successional rate.

Floodplains are the least known and the most threatened of the Amazonian ecosystems. The continuous exploitation of this environment has a long history, but little research has been performed targeting the spatial and temporal effects of human and natural disturbances. Satellite imagery coupled with aerial photos and GIS has proven to be a valuable tool for identifying and analyzing natural and human disturbances. Identifying and classifying changes helps to provide a better understanding of the dynamics of floodplain environments, which is needed for the development of better resource management in these ecosystems.

Acknowledgments

The authors would like to acknowledge funding for this research from the Andrew W. Mellon Foundation and the University of New Hampshire Agricultural Experiment Station under MacIntire-Stennis Grant MS-33. This publication is Scientific Contribution Number 2110 from the New Hampshire Agricultural Experiment Station. The authors would also like to thank the two anonymous reviewers whose comments helped improve this paper.

References

Anderson, A., 1991. Forest management strategies by rural inhabitants in the Amazon estuary, *Rain Forest Regeneration and Management., Man and the Biosphere Series*, Parthenon Publishing, London, United Kingdom, 6(23):351–360.

Anderson, A., I. Mousasticoshvily, and D. Macedo, 1992. *Impactos ecológicos e sócio-econômicos da exploração seletiva de virola no estuário Amazônico. Implicacões Para Politicas Florestais Brasileiras*, World Wildlife Fund?, 185 p (in Portuguese).

Anderson, A.B., and E.M. Ioris, 1992. Valuing the rain forest: Economic strategies by small-scale forest extractivists in the Amazon estuary, *Human Ecology*, 20(3):337–369.

Applegate, B., D. Zarin, and F. Rabelo, 2000. Log and sawn lumber volume relationships for *Calycophyllum spruceanum*: A naturally regenerating timber resource from Amazonian tidal floodplain forest, Amapa-Brazil, *Revista de Ciências Agrárias*, 33:87–96 (in Portuguese).

Barros, C., and C. Uhl, 1995. Logging along the Amazon River and estuary: Patterns, problems and potential, *Forest Ecology and Management*, 77:87–105.

Brondizio, E., E. Moran, P. Mausel, and Y. Wu, 1994. Land use change in the Amazon estuary: Patterns of caboclo settlement and landscape management, *Human Ecology*, 22(3):249–278.

———, 1996. Land cover in the Amazon estuary: Linking of the thematic mapper with botanical and historical data, *Photogrammetric Engineering & Remote Sensing*, 62(8):921–929.

Campbell, J.B., 1987. *Introduction to Remote Sensing*, The Guilford Press, New York, N.Y., 551 p.

Congalton, R.G., 1991. A review of assessing the accuracy of classifications of remotely sensed data, *Remote Sensing of Environment*, 37:35–46.

Congalton, R., and K. Green, 1999. *Assessing the Accuracy of Remotely Sensed Data: Principles and Practices*, CRC/Lewis Press, Boca Raton, Florida, 137 p.

ERDAS, 1995. *Field Guide*, ERDAS Inc., Atlanta, Georgia, 627 p.

ESRI, 1994. *Arc/Info Software Documentation*, Environmental Systems Research Institute, Inc., Redlands, California (software).

Gallopin, G.C., and M. Winograd, 1995. Ecological prospective for Tropical Latin America, *The Fragile Tropics of Latin America: Sustainable Management of Changing Environments*, United Nations University Press, pp. 13–44.

Goulding, M., N. Smith, and D. Mahar, 1996. *Floods of Fortune. Ecology & Economy along the Amazon*, Columbia University Press, New York, N.Y., 193 p.

Hess, L., J. Melack, S. Filoso, and Y. Wang, 1995. Delineation of inundated area and vegetation along the Amazon floodplain with the

SIR-C synthetic aperature radar, *IEEE Transactions on Geoscience and Remote Sensing*, 33:896–904.

IBGE, 1994. *Mapa topográfico do Estado do Amapá.*

INPE, 1990. *Deforestation in Brazilian Amazonia*, Intituto Nacional de Pesquisas Espaciais (INPE), Sao Josē dos Campos, São Paulo, Brazil, 198 p. (in Portuguese).

Jensen, J.R., 1995. *Introductory Digital Image Processing. A Remote Sensing Pespective*, Second Edition, (Prentice Hall series in Geographic Information Science), Prentice-Hall, Englewood Cliffs, New Jersey, 316 p.

Junk, W.J., 1989. The use of Amazonian floodplains under an ecological perspective, *Interciencia*, 14(6):317–322.

Lillesand, T.M., and R. Kiefer, 1994. *Remote Sensing and Image Interpretation, Third Edition*, John Wiley & Sons, Inc., New York, N.Y., 750 p.

Macedo, D.S., and A.B. Anderson, 1993. Early ecological changes associated with logging in an Amazon floodplain., *Biotropica*, 25(2):151–163.

Nelson, B., 1994. Natural forest disturbance and change in the Brazilian Amazon, *Remote Sensing Reviews*, 10:105–125.

Nepstad, D., I. Brown, L. Luz, A. Alechandra, and V. Viana, 1992. Biotic impovrishment of Amazonian forests by rubber tappers, loggers, and cattle ranchers, *Advances in Economic Botany*, 9:1–14.

Onis, J., 1992. *The Green Cathedral*, Oxford University Press, London, England, 280 p.

Paine, D.P., 1981. *Aerial Photography and Image Interpretation for Resource Management*, John Wiley & Sons, Inc., New York, N.Y., 571 p.

Peters, C.M., 1992. The ecology and economics of oligarchic forests, *Advances in Economic Botany*, 9:15–22.

Pinedo-Vasquez, M., D. Zarin, K. Coffey, C. Padoch, and F. Rabelo, *2002*. Post-boom logging in Amazonia, *Human Ecology* (in press.).

Pires, J.M., 1974. Tipos de Vegetação da Amazônia, *Brasil Florestal*, 5(17):48–60 (in Portuguese).

Pollak, H., M. Mattos, and C. Uhl, 1995. A profile of palm heart extraction in the Amazon estuary, *Human Ecology*, 23:357–385.

Prance, G.T., 1979. Notes on the vegetation of Amazonia III. The terminology of Amazonian forest types subject to inundation, *Brittonia*, 31(1):26–38.

Projeto RADAM, 1974. Mapa Exploratório de solos, Folha 22.

Roosevelt, A.C., 1991. *Moundbuilders of the Amazon. Geophysical Archaeology of Marajo Island, Brazil*, Academic Press, New York, N.Y., 495 p.

Roosevelt, A.C. (editor), 1995. *Amazonian Indians from Pre-History to the Present*, The University of Arizona Press, Tucson, Arizona, 462 p.

Sippel, S.J., S.K. Hamilton, J.M. Melack, and E.M. Novo, 1998. Passive microwave observations of inundation area and area/stage relation in the Amazon River Basin, *International Journal of Remote Sensing*, 19:3055–3074.

Skole, D.L., and C. Tucker, 1993. Tropical deforestation and habitat fragmentation in the Amazon: Satellite data from 1978 to 1988, *Science*, 260:1905–1910.

Skole, D.L., W. Chomentowski, W. Salas, and A. Nobre, 1994. Physical and human dimensions of deforestation in Amazonia, *BioScience*, 44(5):314–322.

Story, M., and R. Congalton, 1986. Accuracy assessment: A user's perspective, *Photogrammetric Engineering & Remote Sensing*, 52(3):397–399.

Zarin, D., A. Duchesne, and M. Hiroaka, 1998. Shifting cultivation on the tidal floodplains of Amazônia: Impacts on soil nutrient status, *Agroforestry Systems*, 41:307–311.

Zarin, D., V. Pereira, H. Raffles, F. Rabelo, M. Pinedo-Vasquez, and R. Congalton, 2002. Landscape changes in tidal floodplains near the mouth of the Amazon River, *Forest Ecology and Management* (in press).

(Received 26 June 2001; accepted 18 September 2001; revised 04 October 2001)